

# Skull and Brain Visualization by Transcranial Sonography System

Takashi Shimizu<sup>1</sup>, Kouki Nagamune<sup>1</sup>, Syoji Kobashi<sup>1</sup>, Katsuya Kondo<sup>1</sup>, Yutaka Hata<sup>1</sup>  
Yuri T. Kitamura<sup>2</sup>, and Toshio Yanagida<sup>2</sup>

<sup>1</sup>Graduate School of Engineering  
Himeji Institute of Technology

2167, Shosha, Himeji, 671-2201, Japan

<sup>2</sup>Graduate School of Frontier Biosciences  
Osaka University

2-2, Yamadaoka, Suita, 565-0871, Japan

taka@comp.eng.himeji-tech.ac.jp

## Abstract

*In conventional transcranial sonography system, available window of skull in adults is limited to the temporal bone. However, by visualizing an intracranial tissue from all angles, it supports to diagnose the disease with high accuracy. Transcranial sonography system with placement free has not been developed. This paper describes skull and intracranial tissue visualization based on anatomical knowledge using ultrasound. Generally, it is difficult to visualize an intracranial tissue from frontal bone (3 - 6 mm) because of large attenuation in skull. To overcome this difficulty, we develop the system whose ultrasonic wave can penetrate the human frontal bone. In our system, we acquire data of an intracranial tissue in animal experiment model. This is made by cattle skull and goma-tofu (soft tissue) placed inside the skull. Using acquired data and this model knowledge, we image the skull and the soft tissue. As a result, our method could visualize skull and soft tissue surface in all data.*

## 1. Introduction

Conventional transcranial sonography system can non-invasively image intracranial blood flow and brain tissue at real-time [1]-[3]. However, skull prevents ultrasound from disclosing a brain anatomy. The main factor is the acoustical mismatch between soft skin and the skull. The acoustic velocity in the skull is about 2800 - 3500 m/s whereas about 1600 m/s in soft skin [4][5]. Additionally, porous layer of the skull prevents ultrasound from penetrating to intracranial tissue. Due to this, the system is applicable to neonates whose skull is not developed. However, in adults, available window of skull is limited to the temporal bone [6]-[8]. Because of the limited size of the window, the obtained information is also limited. Any transcranial sonography system with placement free has not been developed. This paper describes intracranial tissue visualization with placement free. By visualizing

shape of an intracranial tissue from all angles, it supports to diagnose the disease with high accuracy.

In Refs. [4], [9], and [10], we confirmed that ultrasonic wave penetrated the human frontal bone (3 - 6 mm) or artificial bone (12 mm).

In this paper, first, we acquire data of an intracranial tissue in animal experiment model. This model is made by cattle skull and goma-tofu (soft tissue). The soft tissue is placed inside the skull. The animal skull and the soft tissue imitate human skull and human brain tissue, respectively. The aim of this experiment is to recognize echoes of skull surface, skull bottom, and soft tissue surface, and to visualize the skull shape and the soft tissue surface. Second, we acquire the data of the model in a water bath. We determine each region position (skull surface, skull bottom, and soft tissue surface) using the anatomical knowledge. Finally, we image the skull and the soft tissue from these positions. As the result of applying it to the model, we could recognize echoes of skull surface, skull bottom and soft tissue surface. The shape of skull and the soft tissue in all data were obtained. Average error of the skull thickness was 0.43 mm, and the average error of water distance between skull bottom and soft tissue surface was 3.14 mm.

This paper organized as follows. Section 2 describes human brain model and overview of our experiment. Section 3 describes the visualization based on the anatomical knowledge. Section 4 shows the experimental result on cattle skull. In it, we could successfully visualize the shape of the skull and the soft tissue. Section 5 presents a summary of the technical results.

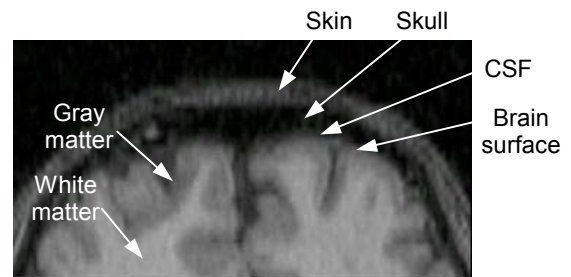
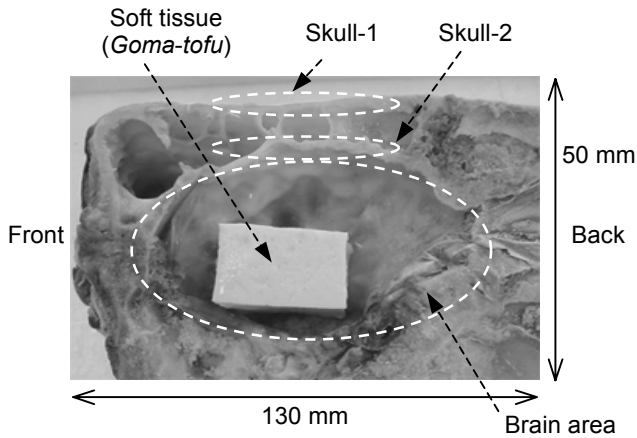
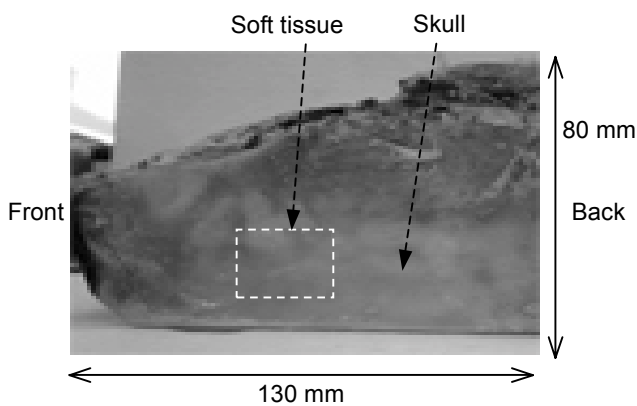


Figure 1. Human brain.



(a) Lateral view.



(b) Top view.

Figure 2. Animal experiment model.

## 2. Preliminary

### 2.1 Human brain model

Figure 1 shows MR image of the human brain. Information of the shape of brain surface in this figure is important to discriminate human disease. Additionally, the human brain consists of the skin (light white), the skull (black), cerebrospinal fluid (black), the gray matter (light black), the white matter (white). We construct animal experiment model using cattle skull and soft tissue. Constructed model is shown in Figure 2. Figure 2(a) shows the model of lateral view. Figure 2(b) shows the model of top view. As shown in Figure 2(a), brain portion is removed and a soft tissue is placed in it. In this model, the soft tissue (*goma-tofu*) is used instead of human brain. The aim of this experiment is to visualize the skull and the soft tissue. Cattle skulls were two layers: skull-1 denotes upper skull and skull-2 denotes lower skull. Skull thickness of the model varies from 2 to 5 mm.

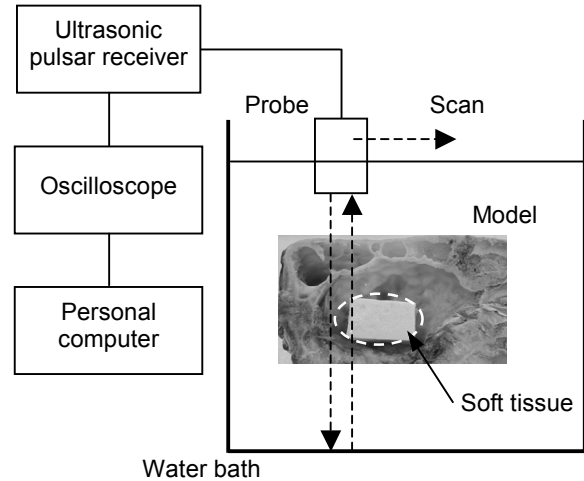


Figure 3. Overview of our experiment.

### 2.2 Overview of our experiment

The animal experiment model is placed into a water bath and we acquire data of the intracranial soft tissue. Figure 3 shows the overview of our experiment. The ultrasonic pulsar receiver (New Sensor Inc., NSI-PR2000L) transmits and receives ultrasonic waves via the probe. The data of ultrasonic waveform is acquired by the personal computer. The data obtained by this system includes the reflected wave from the skull surface, skull bottom, and intracranial soft tissue. Sampling interval is 10ns. We determined transmission frequency that is suitable for the skull penetration as 1MHz [4][9][10]. Additionally, in order to visualize intracranial soft tissue, we used ultrasonic focus probe (KGK, 1.0K14I/6I-F20) whose center frequency is 1MHz. We scan at interval of 1 mm using scanner equipment, and acquire data from above animal skull in each position. Scan field of probe is 60 mm and sixty-one data is acquired. An image consists of sixty-one data.

### 3. Visualization method based on the anatomical knowledge

This section describes model visualization method based on the anatomical knowledge. We perform visualization of human brain model by the following process.

- (1) Determine each region position (skull-1 surface, skull-1 bottom, skull-2 surface, skull-2 bottom, and soft tissue surface) using the knowledge of model structure,
- (2) Determine these positions considering the ultrasound velocity,
- (3) Visualize these positions.

The detail of each process is as follows.

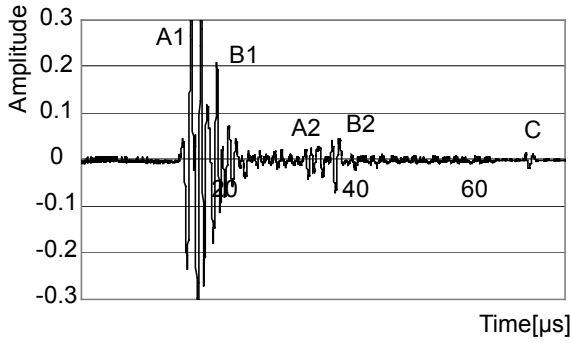


Figure 4. Ultrasonic waveform.

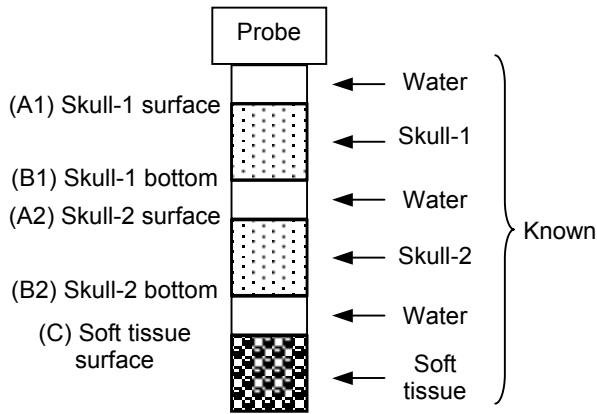
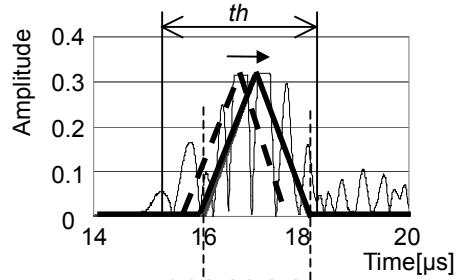


Figure 5. Model structure.

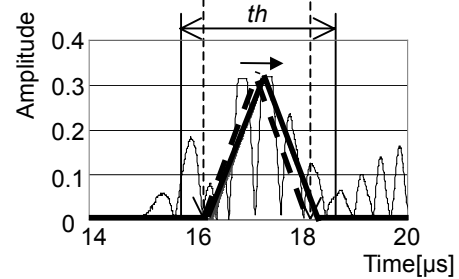
### 3.1 Determination of each region position

Figure 4 shows an example of ultrasonic waveform which is acquired in Figure 3. Path of each reflected wave (A1, B1, A2, B2, and C) is automatically determined. As shown in Figure 5, the model consists of layer structure in order: water, skull-1, water, skull-2, water, and soft tissue. We can therefore assume that these reflected waves are acquired in the order of skull-1 surface, skull-1 bottom, skull-2 surface, skull-2 bottom, and soft tissue surface. Therefore, in Figure 4, A1 represents reflected wave of skull-1 surface, B1 represents reflected wave of skull-1 bottom, A2 represents reflected wave of skull-2 surface, B2 represents reflected wave of skull-2 bottom, and C represents reflected wave of soft tissue surface. They are shown in Figure 5. Path of each reflected wave of sixty-one data is also automatically determined using the knowledge of model shape. The details are below.

Figure 6 shows the method of position determination of skull-1 surface. First, for first data of sixty-one data, we manually determine position of skull-1 surface as the initial position. A triangle function of the initial position is expressed by dotted line in Figure 6(a). The triangle function is shown in Figure 7. The function moves the range of threshold,  $th=3 \mu s$ . The triangle function is used



(a) Initial data.



(b) Next data.

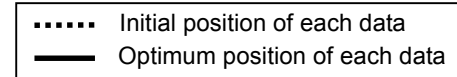


Figure 6. Position determination of region.

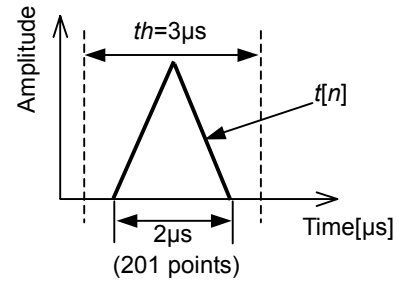


Figure 7. Triangle function.

for calculating the function  $S_i$ . The function  $S_i$  is defined by Equation (1).

$$S_i = \sum_{n=-100}^{100} x[n+i] \cdot t[n] \quad (1)$$

where,  $x[n]$  denotes modulus of original signal,  $t[n]$  denotes triangle function. We calculate  $S_i$  for all  $i$  ( $15.0 \mu s \leq i \leq 16.0 \mu s$ ). Position of triangle function with maximum  $S_i$  is determined as the optimum position of skull-1 surface of the first data. Triangle function of optimum position is expressed by solid line.

Second, as shown in Figure 6(b), the optimum position of initial data is applied to the initial position of next data (second data). This is why the region position is approximately same in the neighboring data. In the similar way, the triangle function is applied to the initial position, and  $S_i$  is calculated for every position  $i$  using

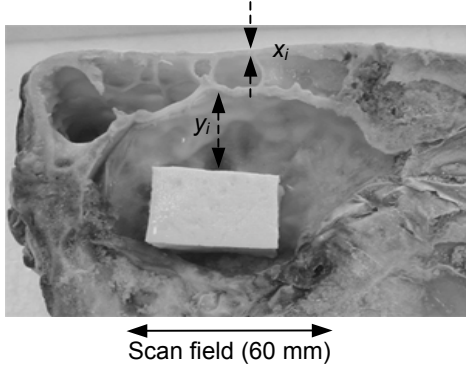


**Figure 8. Calculation of real value (lateral view).**

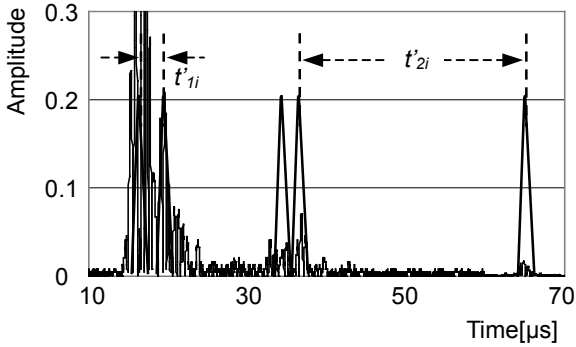


**Figure 9. Time difference.**

Equation (1). The optimum position of skull-1 surface for second data is determined. After performing above process to all sixty-one data in order, the positions of skull-1 surface are determined.

Finally, region position of skull-1 bottom, skull-2 surface, skull-2 bottom, and soft tissue surface are determined.

### 3.2 Determination of positions considering the ultrasound velocity

Horizontal axis of Figure 4 is time axis. We calculate distances from time-amplitude plane. First, we measure skull-1 thickness  $x_i$  and water distance  $y_i$  between skull-2 bottom and soft tissue surface in Figure 8. They are assumed as the real values. Second, we estimate skull-1 thickness  $x'_i$  and water distance  $y'_i$  between skull-2 bottom and soft tissue surface from positions of the determined triangle function, respectively. Suffix  $i$  denotes the number of scan data. As  $x'_i$  denotes skull-1 thickness, as shown in Figure 9, we calculate time difference  $t'_{1i}$  between skull-1 surface and skull-1 bottom. We define  $x'_i$  by Equation (2).

$$x'_i = \frac{1}{2} t'_{1i} \times v'_i \quad (2)$$

where,  $v'_i$  is acoustic velocity. We assume that ultrasound velocity in skull is 3100 m/s. On the other hand, time

difference of  $y'_i$  is  $t'_{2i}$  between skull-2 bottom and soft tissue surface. We define  $y'_i$  by Equation (3).

$$y'_i = \frac{1}{2} t'_{2i} \times v'_i \quad (3)$$

We assume that ultrasound velocity in water is 1480 m/s [4][10][11]. We visualize these distances using this value  $x'_i$  and  $y'_i$ . Thus, we visualize points of all estimated distances.

## 4. Experimental results

In our experiment, we acquired data of three lines as shown in Figure 10. Sixty-one data is acquired in each line, and construct an image. These results are shown in Figure 11. In all figures, lines A1 and B1 represent skull-1 surface and skull-1 bottom, respectively. Line C represent soft tissue surface. We could recognize skull-1 surface and skull-1 bottom, and could confirm soft tissue surface form all image. Consequently, our system could visualize skull-1 shape and intracranial soft tissue from every position.

Figure 12 visualizes an overlapped image of Figures 2(a) and 11 (a). In it, extracted line exactly matched to the skull boundaries and soft tissue surface.

Figure 13 show a comparison between real thickness and calculated thickness for 1st line. The  $x_i$  is real value of skull-1 thickness and  $x'_i$  is the calculated value of skull-1 thickness by our method. The  $y_i$  is real value of water distance and  $y'_i$  is the calculated value of water distance by our method. Average of  $x_i$  was 3.52 mm and average of  $x'_i$  was 3.16 mm. The calculated value of skull thickness was smaller than real value. Average of  $y_i$  was 27.93 mm and average of  $y'_i$  was 29.47 mm. The calculated value of water distance was larger than real value. We could visualize the skull and soft tissue with average error 0.38 mm and 2.94 mm, respectively. Average error  $x_{err}$  of skull-1 thickness and  $y_{err}$  of water distance are calculated by Equations (4) and (5), respectively.

$$x_{err} = \sum_i^n |x_i - x'_i| / n \quad (4)$$

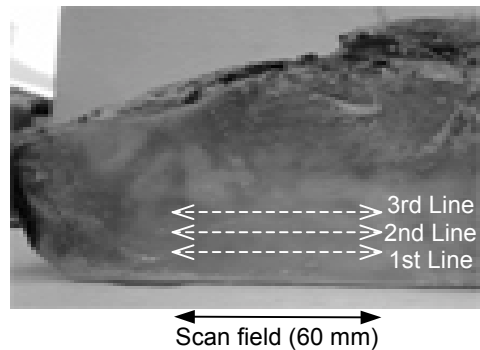


**Figure 10. Data acquisition line (top view).**

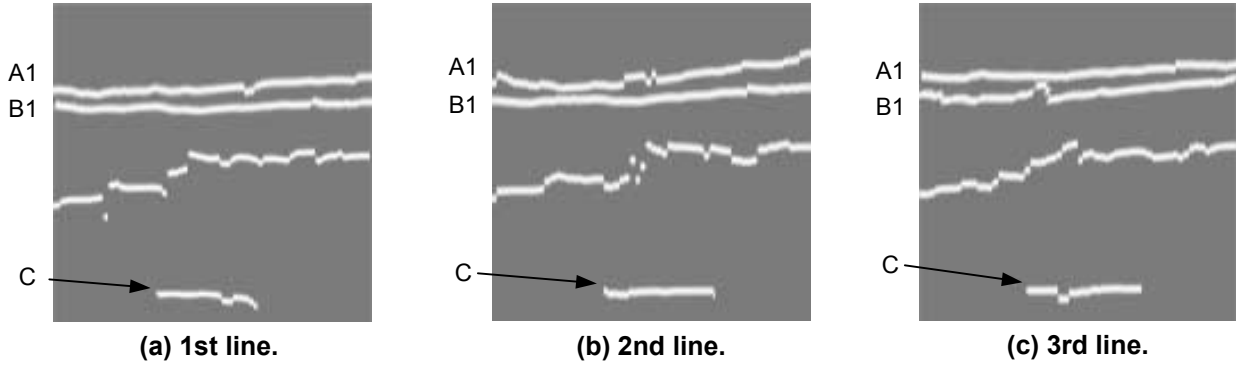


Figure 11. Experimental result.

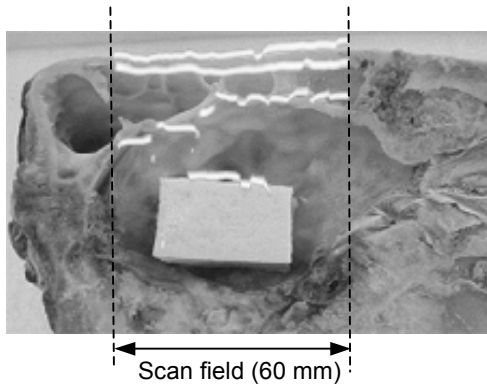


Figure 12. Overlapped result.

Table 1. Average error of all results.

| Line    | Animal skull thickness $x_{err}$ |                    | Water distance $y_{err}$ |                    |
|---------|----------------------------------|--------------------|--------------------------|--------------------|
|         | Average                          | Standard deviation | Average                  | Standard deviation |
| 1       | 0.38                             | 0.31               | 2.94                     | 1.27               |
| 2       | 0.35                             | 0.26               | 3.11                     | 1.10               |
| 3       | 0.55                             | 0.33               | 3.38                     | 1.53               |
| Average | 0.43                             | 0.59               | 3.14                     | 1.30               |

(Unit [mm])

$$y_{err} = \sum_i^n |y_i - y'_i| / n \quad (5)$$

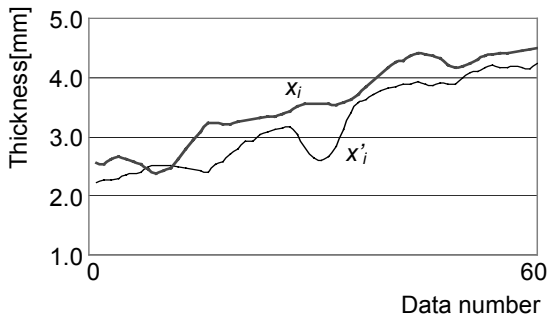
where,  $n$  denotes number of data.

Table 1 tabulates average error in each line. In skull thickness, 2nd line has the lowest average error with 0.35 mm. In water distance, 1st line has the lowest average error with 2.94 mm. Average error of skull thickness is 0.43 mm and average error of water distance is 3.14 mm for all lines.

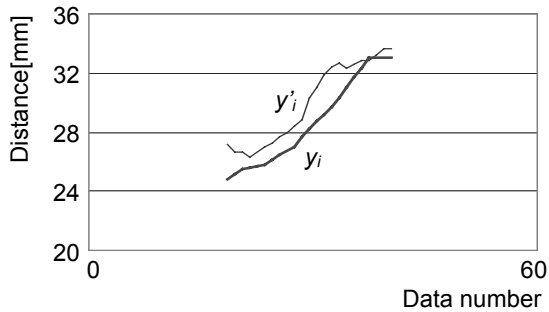
## 5. Conclusion

In this paper, we have proposed a visualization method of skull and brain tissue using ultrasound. In it, we constructed the human brain model using the cattle skull and soft tissue. This method employs that a path of each echo is uniquely derived from order of model structure. We applied this method to the cattle skull and soft tissue. This cattle skull thickness varies from 2 to 5 mm. We acquired three line data along different line. We could visualize the skull and the soft tissue for all lines. The average error of skull thickness and water distance were 0.43 mm and 3.14 mm, respectively. By considering thickness of the human skull is from 3 to 6 mm, our system could visualize human brain from all angles.

It remains as a future work to apply our method to human head.



(a) Skull-1 thickness.



(b) Water distance.

Figure 13. Evaluation result of 1st example.

## Acknowledgement

This work was supported in part by the Ministry of Education, Culture, Sports, Science and Technology, Grant-in-Aid for Scientific Research (B) (KAKENHI 14370284) 2001.

## References

- [1] C. R. Levi, C. Selmes, and B. R. Chambers, "Transcranial Ultrasound Clinical Applications in Cerebral Ischaemia," *Australian Prescriber*, 24(6):137-140, 2001.
- [2] G. Becker, "Perspectives of Cerebral Sonography in Neurology," *Electromedica*, 68:Neuro, 21-26, 2000.
- [3] W. Hirsch, W. Hiebsch, H. Teichler, and A. SchIuter, "Transcranial Doppler Sonography in Children: Review of a Seven-Year Experience", *Clinical Radiology*, 57(6):492-497, June. 2002.
- [4] K. Nagamune, S. Kobashi, K. Kondo, Y. Hata, Y. T. Kitamura, and T. Yanagida, "Challenge to the Development of a Transcranial Sonography System," *Proc. 6th Int. Conf. on Knowledge-Based Intelligent Information Engineering Systems & Allied Technologies*, 604-608, September. 2002.
- [5] J. Ylitalo, and J. Koivukangas, "Ultrasonic Echo Tomography Trough Skullbone," *Ultrasonics Symposium*, 1019-1022, 1989.
- [6] L. L. Berland, C. R. Bryan, and B. C. Sekar, "Sonographic Examination of the Adult Brain," *J. Clin. Ultrasound*, 337-345, 1988.
- [7] G. Becker, A. Krone, D. Koulis, A. Lindner, E. Hofmann, W. Roggendorf, and U. Bogdahn, "Reliability of Transcranial Colourcoded Real-Time Sonography in the Assessment of Brain Tumors: Correlation between Ultrasound, Computerized Tomography and Biopsy Findings," *Neuroradiology*, 36:585-590, 1994.
- [8] D. Berg, and G. Becker, "Perspectives of B-Mode Transcranial Ultrasound," *NeuroImage*, 15:463-473, 2002.
- [9] Y. Hata, T. Shimizu, S. Kobashi, K. Kondo, Y. T. Kitamura, and T. Yanagida, "A Fuzzy Logic Approach to Transcranial Sonography System with Placement Free," *Proc. 1st Int. Conf. on Information Technology & Applications*, CD-ROM, November. 2002.
- [10] T. Shimizu, K. Nagamune, S. Kobashi, K. Kondo, Y. Hata, Y. T. Kitamura, and T. Yanagida, "An Automated Ultrasound Discrimination System of Tissue under an Obstacle by Fuzzy Reasoning," *Joint. 1th Int. Conf. on Soft Computing and Intelligent Systems*, 83, October. 2002.
- [11] J. Krautkramer, and H. Krautkramer, *Ultrasonic Testing of Materials*, 4<sup>th</sup> fully revised Edition, 1990.